

<https://doi.org/10.1038/s41612-024-00619-z>

# A warming climate will make Australian soil a net emitter of atmospheric CO<sub>2</sub>

R. A. Viscarra Rossetl<sup>1</sup>✉, M. Zhang<sup>1</sup>, T. Behrens<sup>2,3</sup> & R. Webster<sup>4</sup>

Understanding the change in soil organic carbon (C) stock in a warmer climate and the effect of current land management on that stock is critical for soil and environmental conservation and climate policy. By simulation modeling, we predicted changes in Australia's soil organic C stock from 2010 to 2100. These vary from losses of 0.014–0.077 t C ha<sup>-1</sup> year<sup>-1</sup> between 2020 and 2045 and 0.013–0.047 t C ha<sup>-1</sup> year<sup>-1</sup> between 2070 and 2100, under increasing emissions of greenhouse gases and temperature. Thus, Australian soil will be a net emitter of CO<sub>2</sub>. Depending on the future socio-economic conditions, we predict that croplands will accrue as much as 0.19 t C ha<sup>-1</sup> year<sup>-1</sup> between 2020 and 2045 due to their management, but accrual will decrease with warming and increased emissions by 2070–2100. The gains will be too small to counteract the losses of C from the larger areas of rangelands and coastal regions that are more sensitive to a warmer climate. In principle, prudent management of the rangelands, for example, improving grazing management and regenerating biodiverse, endemic native plant communities, could sequester more C and mitigate the loss; in practice, it may be more difficult, requiring innovation, interdisciplinary science, cultural awareness and effective policies.

The Earth's soil is a crucial component of the global carbon (C) cycle. Its immense C store<sup>1–3</sup> and concerns about the effects of a warming climate on its stability have forced scientists and politicians to take serious note of the soil<sup>4</sup>. Small changes in the soil's C store can significantly affect the terrestrial C cycle. Understanding the effects of climate change on the soil's C dynamics is therefore crucial for land management, adaptation to a warming climate, and mitigation in the medium- (2045–2070) and long-term (2070–2100).

It is generally agreed that the Earth has warmed by approximately 1°C in the last 100 years, mainly due to increased CO<sub>2</sub> emissions from industry and transport. A further increase to 1.5°C above preindustrial temperature is expected within the foreseeable future unless we can reduce emissions and remove greenhouse gases from the atmosphere<sup>5</sup>. Delegates at COP27, although wishing to limit the increase to 1.5°C by 2050, failed to agree on cuts in emissions to achieve that goal. Worse, if emissions continue at the current rate, an increase to 2°C is likely sometime this century. Such warming is predicted to have dire consequences and potentially catastrophic impacts on humankind, the environment, and the economy. The warnings have been repeated by scientists, and many politicians, too, are now treating

them seriously. If we are to restrict global warming beyond 1.5°C then we need to limit the net increase in CO<sub>2</sub> in the atmosphere to zero, together with substantial reductions in the emissions of other greenhouse gases such as methane and nitrous oxide. Therefore, scientists, stakeholders, and politicians are considering the capture and storage of greenhouse gases (GHG) and C sequestration to achieve 'net zero' emissions.

The capture and storage of CO<sub>2</sub> at sources from industry and power stations is a matter of technology. That from the atmosphere must depend on nature, by photosynthesis and on land by storing C in the soil. Soil and vegetation currently absorb roughly one-third of global anthropogenic emissions<sup>3</sup>. The soil's capacity to sequester C could be increased by changing land use, conservation, restoration, and sound soil management. These 'Nature-based' actions, aided by modern technologies, could be implemented immediately and cost-effectively to limit the effects of climate change<sup>6</sup>. Unlike the C stored in vegetation, C in the soil is more resilient to fire, pests, and wind, providing a medium for plant growth and ecosystem services, such as greater water storage and reduced runoff, erosion and flooding, landscape rehabilitation, food security and sustainable development<sup>7</sup>.

<sup>1</sup>Soil & Landscape Science, School of Molecular & Life Sciences, Faculty of Science & Engineering, Curtin University, GPO Box U1987, Perth, WA 6845, Australia.

<sup>2</sup>Soil and Spatial Data Science, Soilution GbR, Heiligegeiststrasse 13, 06484 Quedlinburg, Germany. <sup>3</sup>Swiss Competence Center for Soils (KOBO), School of Agricultural, Forest and Food Sciences (HAFL), Bern University of Applied Sciences, Länggasse 85, 3052 Zollikofen, Switzerland. <sup>4</sup>Rothamsted Research, Harpenden AL5 2JQ, UK. ✉e-mail: [r.viscarra-rossel@curtin.edu.au](mailto:r.viscarra-rossel@curtin.edu.au)

The Coupled Model Intercomparison Project Phase 6 (CMIP6) predicts that in Australia, temperature and the concentration of CO<sub>2</sub> in the atmosphere will continue to increase, precipitation will become more variable, and these together will cause significant changes in the terrestrial C cycle<sup>8</sup>. The CMIP6 also forecasts that a warming climate will cause more frequent heat waves, fires, and droughts<sup>9</sup>, which could result in losses of C from the soil, with long-lasting effects on C cycling<sup>10</sup>. That, coupled with mismanagement of the land, would make the storage of C in the soil and vegetation less likely, and ultimately, it would release much of the stored C to the atmosphere as CO<sub>2</sub>. This, in turn, would exacerbate climate change. Despite the current discussion, however, we have yet to determine whether the soil will act as a sink or source of atmospheric CO<sub>2</sub> in the future.

Australian soil holds 27.95 Gt C in its uppermost 30 cm layer<sup>11</sup>. The soil for arable cropping and grazing on modified pastures holds approximately 16% of the C stock. The soil of the rangelands contains relatively little C, on average 27 t ha<sup>-1</sup>. Nevertheless, because rangelands are vast and occupy around 80% of the continental land area, it remains Australia's largest store of terrestrial C with ≈ 70% of the total C stock<sup>12</sup>, which is more than the estimated 7–15 Gt of all above-ground C in these regions<sup>13</sup>. Land clearing for agriculture and pastoralism by European settlers over the past 230 years in Australia has caused overgrazing and degradation. It has been the primary cause of the soil's loss of C since. Conversion of native vegetation to agriculture has decreased the stocks of organic C in the soil by 20–70%<sup>14,15</sup>. However, uncertainty remains about the potential of soil in Australia to store C, the rate of C accumulation, and its permanence. Under a warmer, drier climate, Australian soil risks becoming a source of C rather than a sink, further enhancing its disproportionate emissions (≈ 1.4% of global emissions) relative to its population (≈ 0.3% of the global population). The scarcity of data and the

lack of understanding of the soil's C dynamics mean there is no consensus on the soil's likely response to future climate change.

Here, we integrate more than 4000 observations of the 0–30 cm total organic C (TOC), the particulate organic C (POC), and mineral-associated organic C (MAOC) with the Rothamsted Carbon Model Roth C<sup>16</sup>, one of the constituent models in Australia's Full Carbon Accounting Model (FullCAM)<sup>17</sup>, under the framework developed by<sup>18</sup>, and explore the effects of climate and C inputs on the C dynamics of Australian soil from 2010 to the year 2100. We aim to assess whether Australia's soil is a sink or a source of atmospheric CO<sub>2</sub> and use climate forcing from an ensemble of six Earth System Models (ESM) from the CMIP6<sup>19,20</sup>, site-specific C inputs, and three shared socioeconomic pathways (SSPs)<sup>21,22</sup>:

SSP1-2.6 represents a 'sustainability' pathway with an expected radiative forcing of 2.6 W m<sup>-2</sup> in 2100. Emissions of GHGs are small, and CO<sub>2</sub> emissions are cut to zero by 2075. Temperatures will increase by 1.7°C between 2040 and 2060 and by 1.8°C between 2080 and 2100.

SSP2-4.5 represents a 'middle-of-the' road scenario with an expected radiative forcing of 4.5 W m<sup>-2</sup> in 2100. Emissions of CO<sub>2</sub> remain until 2050 approximately as now and then decrease, eventually reaching zero in 2100. Temperatures are assumed to increase by 2.0°C between 2040 and 2060 and 2.7 °C between 2080 and 2100.

SSP5-8.5 represents 'fossil-fueled development', with an expected radiative forcing of 8.5 W m<sup>-2</sup> in 2100. It includes significant GHG emissions, particularly a tripling of CO<sub>2</sub> emissions by 2075, and estimated warming of 2.4°C between 2040 and 2060 and 4.4 °C between 2080 and 2100<sup>8</sup>.

## Results

Australia's climate to the end of the century is predicted to become warmer and drier (Fig. 1). The vast rangelands—arid to semi-arid and seasonally

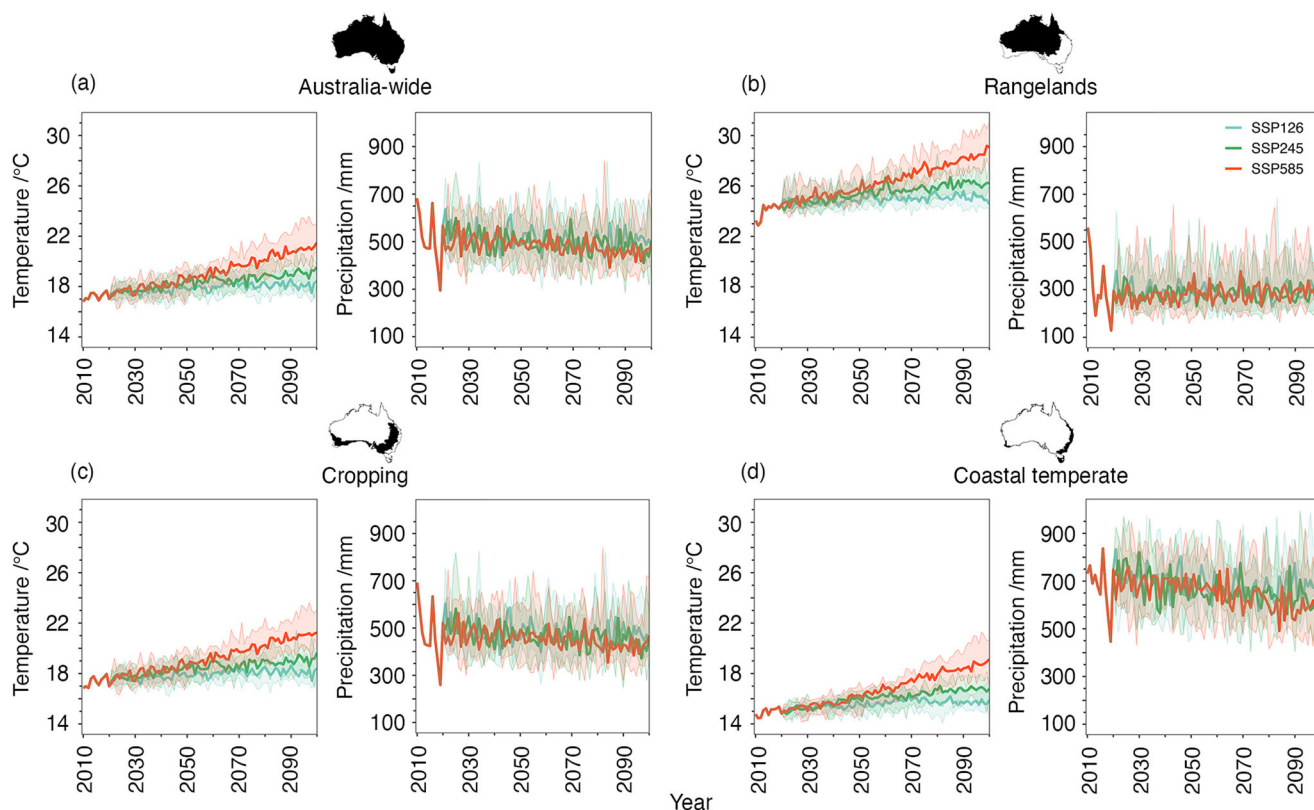


**Fig. 1 | Predicted median temperature and precipitation from the year 2010 to 2100. a** Median temperature and precipitation over all of Australia, **b** the rangelands, **c** cropping regions, and **d** coastal temperate regions, for the three shared socio-economic pathways (SSP): SSP1-2.6 represents 'sustainability', SSP2-

4.5 'middle-of-the-road', and SSP5-8.5 'fossil-fueled development' scenarios. The shaded ribbons represent the interdecile range of the predictions made with the six Earth System Models (see "Methods", Table 3).

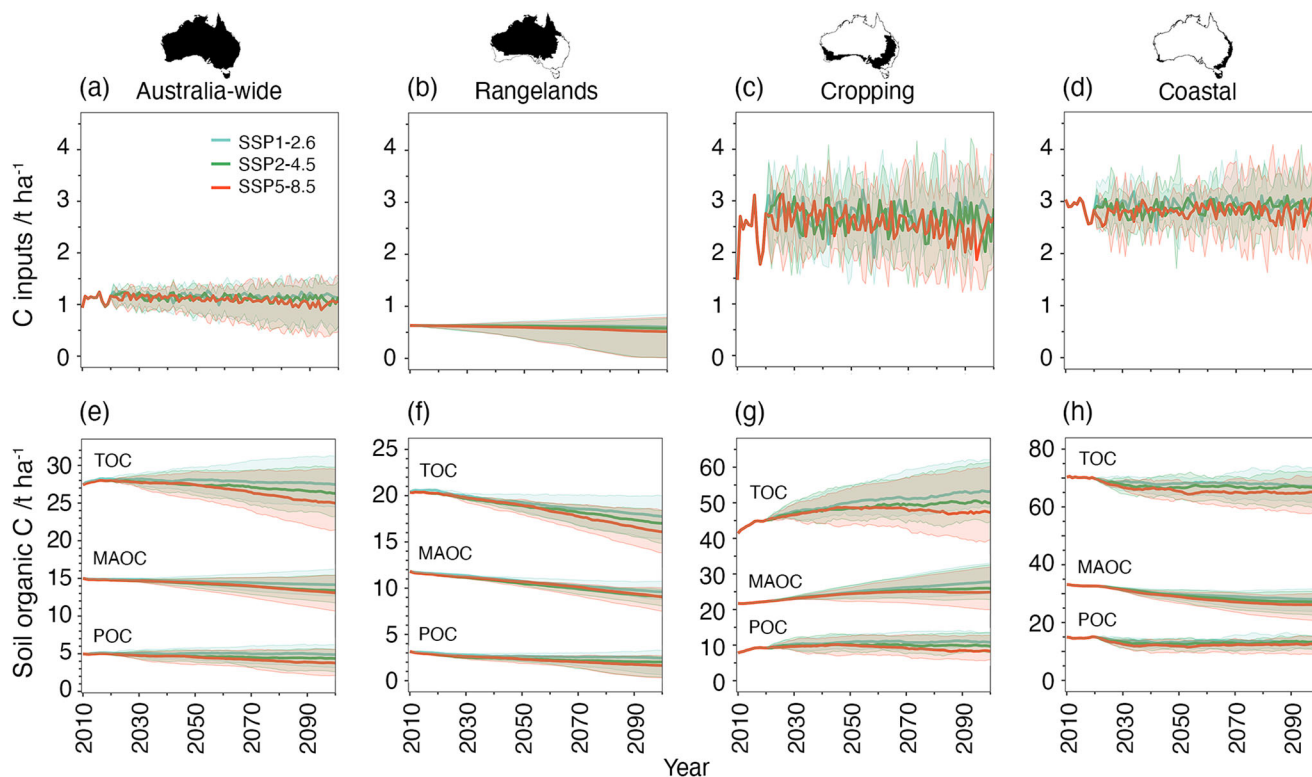


**Fig. 2 | Predicted median carbon inputs (C inputs) and soil organic C from 2010 to 2100. a–d** C inputs and **e–h** total soil organic C (TOC), mineral-associated organic C (MAOC), and particulate organic C (POC), over all of Australia (**a, e**), the rangelands (**b, f**), cropping regions (**c, g**) and coastal temperate regions (**d, h**), for the

three shared socio-economic pathways (SSP): SSP1-2.6 represents ‘sustainability’, SSP2-4.5 ‘middle-of-the-road’, and SSP5-8.5 ‘fossil-fueled development’ scenarios. The shaded ribbons represent the interdecile range of the predictions made with the six Earth System Models (see ‘Methods’, Table 3).

high rainfall regions—will warm more than other areas. Changes in the amount and distribution of rain remain uncertain, but rainfall is more likely to increase in the wet season in the northern rangelands. In contrast, the southern rangelands will generally have less rain in winter and spring, and the number of dry days will increase<sup>23</sup>. Regions under cropping will warm more slowly than the rangelands, and precipitation will decrease more slowly (Fig. 1). Coastal temperate regions will warm less than the rangelands and cropping regions (Fig. 1). The coastal temperate region has the largest annual rainfall both now and predicted in 2100. Though the predictions are uncertain, precipitation will generally decrease, and the area will become more susceptible to drying (Fig. 1).

**Soil carbon dynamics**

The Roth C framework we used to predict changes in soil C<sup>18</sup> enables a data-driven initialization of the model using POC and MAOC measurements, which represent the model’s primary pool structure<sup>16</sup>. Therefore, we did not need spin-up simulations (i.e. simulations until the model reaches equilibrium). This meant that we could effectively run the simulations at any site with its particular conditions in Australia to predict the effects of climate and management on the soil’s C dynamics (see ‘Methods’).

We derived C inputs separately for the rangelands, cropping (including modified grazing), and coastal regions and then combined the results to obtain the Australia-wide C inputs (see Methods). The simulated median annual C inputs across Australia increase from the baseline period and remain relatively constant under SSP1-2.6. Under SSP2-4.5, however, the C inputs decrease steadily, and faster under SSP5-8.5 (Fig. 2a). The median change in C inputs relative to the  $\approx 1 \text{ t ha}^{-1}$  at the baseline tends to decline into the future, and it is smallest under SSP5-8.5 (Table 1). The TOC stock of Australian soil at the baseline was  $27.4 \text{ t ha}^{-1}$ , and until 2020, we predict that the soil gained on average  $\approx 0.7 \text{ t ha}^{-1}$  organic C (Fig. 2e). The gain can be attributed to wetter years, for example, from a prolonged La Niña period and

enhanced productivity<sup>24</sup> with concomitant increases in C inputs and POC production.

Under SSP1-2.6, the predicted TOC stock in 2020 is  $28.1 \text{ t ha}^{-1}$ , decreasing slightly to 2050 and then more rapidly by  $\approx 0.5 \text{ t ha}^{-1}$  until 2100 (Fig. 2e). Relative to the baseline, under SSP2-4.5 and SSP5-8.5 the change in TOC will also remain positive, but only until 2050. After that, we predict that Australian soil will, on balance, lose C faster under SSP2-4.5 and SSP5-8.5, respectively (Fig. 2e). Here, the predicted C inputs will not compensate the climate-driven C losses, needing C inputs of more than  $\approx 1.2 \text{ t ha}^{-1}$  to compensate for the soil C loss due to the  $\approx 1.4^\circ\text{C}$  change in temperature (Fig. 2, Table 1, Fig. 1). The median loss under SSP2-4.5 relative to the baseline will be  $0.68 \text{ t ha}^{-1}$  by 2070–2100 (Table 1). Our simulations with Roth C show that the loss of MAOC and its loss rate will be greater than that of POC, which is replenished by the addition of C from plants (Fig. 2e).

We derived C inputs for the rangelands by adjusting the rate of change in NPP from the ESM ensemble, which accounts for the fertilization effect of CO<sub>2</sub> (see Methods). Carbon inputs per unit area in the rangelands are small and at the baseline are a little more than  $\approx 0.5 \text{ t ha}^{-1}$  (Fig. 2b). We predict that the median C input change will decrease slightly and steadily between now and 2100 (Table 1). Although increases in CO<sub>2</sub> are likely to provide positive responses in plant growth in the rangelands<sup>25</sup>, the decreased productivity in the warmer climate appears to counteract any gains from that potential growth. Relative to the baseline, soil in the rangelands will lose organic C (Fig. 2f), with average predicted losses by 2020–2045 of  $0.51 (\pm 0.49) \text{ t ha}^{-1}$  under SSP1-2.6,  $0.80 (\pm 0.34) \text{ t ha}^{-1}$  under SSP2-4.5 and  $0.70 (\pm 0.67) \text{ t ha}^{-1}$  under SSP5-8.5. The loss is more significant with increased warming by 2045–2070 and greater by 2070–2100 (Table 1). Both the loss of MAOC and its loss rate are greater than that of the POC (Fig. 2f). The implications are important because small losses per unit area over the vast extent of the rangelands will significantly affect soil C sequestration and accrual in Australia as a whole.

**Table 1 | Predicted median changes in carbon inputs (C inputs) and total organic carbon (TOC) relative to the 1990–2010 baseline, for 2020–2045, 2045–2070 and 2070–2100, in tonnes per hectare**

Scenario	C inputs / t ha <sup>-1</sup>			TOC / t ha <sup>-1</sup>		
	SSP1-2.6	SSP2-4.5	SSP5-8.5	SSP1-2.6	SSP2-4.5	SSP5-8.5
Year	Australia-wide					
2020–2045	0.22 (0.29)	0.23 (0.30)	0.21 (0.31)	0.70 (1.29)	0.33 (1.21)	0.27 (1.35)
2045–2070	0.23 (0.44)	0.20 (0.43)	0.17 (0.47)	0.60 (2.78)	– 0.09 (2.57)	– 0.37 (2.96)
2070–2100	0.22 (0.57)	0.18 (0.57)	0.11 (0.74)	0.28 (4.31)	– 0.68 (4.26)	– 1.96 (4.77)
	Rangelands					
2020–2045	– 0.01 (0.11)	– 0.01 (0.10)	– 0.02 (0.13)	– 0.51 (0.49)	– 0.8 (0.34)	– 0.7 (0.67)
2045–2070	– 0.01 (0.27)	– 0.02 (0.25)	– 0.05 (0.33)	– 1.39 (1.79)	– 1.75 (1.33)	– 1.85 (1.59)
2070–2100	– 0.01 (0.47)	– 0.04 (0.46)	– 0.10 (0.55)	– 2.15 (3.09)	– 2.85 (2.59)	– 3.51 (2.91)
	Cropping					
2020–2045	1.25 (0.88)	1.30 (0.98)	1.25 (0.90)	6.47 (3.5)	5.9 (3.58)	5.58 (3.30)
2045–2070	1.30 (1.02)	1.18 (1.08)	1.16 (1.01)	9.37 (6.2)	7.43 (6.29)	7.18 (7.28)
2070–2100	1.23 (1.04)	1.13 (1.14)	0.99 (1.41)	10.86 (8.2)	8.54 (9.05)	6.05 (11.18)
	Coastal					
2020–2045	– 0.14 (0.55)	– 0.20 (0.57)	– 0.22 (0.53)	– 1.74 (3.83)	– 2.86 (4.1)	– 3.81 (3.72)
2045–2070	– 0.06 (0.58)	– 0.16 (0.59)	– 0.21 (0.62)	– 2.02 (4.75)	– 3.22 (6.29)	– 5.12 (6.18)
2070–2100	– 0.07 (0.59)	– 0.13 (0.69)	– 0.23 (1.01)	– 2.42 (7.43)	– 3.56 (8.19)	– 5.32 (7.84)

Values in brackets represent interdecile ranges.

C inputs to cropland soil and the coastal temperate regions were derived with a crop growth model parameterised with data on agricultural activities that are linked to crop type at the Statistical Area Level 2 (SA2) regions (see “Methods”). We assumed that the crops were grown in rotations and used agricultural activity data to determine the rotations by identifying the three most common crops or grasses at each site in a particular SA2 region (Fig. 3; see “Methods”). We then conducted the simulations at each site with the three crop or grass types using six different climate models for each SSP scenario. This helped to simulate potential crop and pasture rotations and to implicitly account for the effect of management practices on the allocation of C inputs to the soil (Fig. 3; see “Methods”). We prioritized the explicit selection of crops and pastures over management [as suggested by Unkovich et al.<sup>26</sup>, for soil C accounting] because in Australia, there has been widespread adoption and implementation of no-till farming since the 1980–1990s<sup>27</sup>, and data on fertilizer use and stubble retention are scarce<sup>26</sup>. We used only one annual or perennial grass species for sites that fell in the coastal temperate region (Fig. 3).

Carbon inputs under SSP1-2.6 will increase until 2050, but under SSP2-4.5 and SSP5-8.5, they will decrease from 2070 onwards (Fig. 2c). Relative to the  $\approx 1.5 \text{ t ha}^{-1}$  baseline, the change in C inputs by 2020–2045 is  $1.25 (\pm 0.88) \text{ t ha}^{-1}$  for SSP1-2.6, remaining relatively constant under the different SSPs, but decreasing to the year 2100 (Table 1). The predicted organic C in cropping soil under SSP1-2.6 increases faster than SSP2-4.5 and SSP5-8.5 (Fig. 2g). Relative to the baseline, we predict that soil under cropping will gain  $6.47 (\pm 3.62) \text{ t ha}^{-1}$  under SSP1-2.6,  $5.90 (\pm 3.63) \text{ t ha}^{-1}$  under SSP2-4.5 and  $5.58 (\pm 3.30) \text{ t ha}^{-1}$  under SSP5-8.5. The accrual decreases with increasing warming and emission scenarios to 2100 (Table 1). The predictions have similar trends for MAOC and POC, but MAOC accumulates more than POC, which is more seasonal and readily decomposed (Fig. 2g).

The C inputs in the coastal temperate region are the largest in Australia; the median annual change in C inputs to 2100 decreases slightly under the three SSPs, and the simulated changes become more uncertain in the future (Fig. 2d). The magnitude of the change in C inputs relative to the  $\approx 3 \text{ t ha}^{-1}$  at the baseline will decrease slightly throughout the simulation, as there are fewer C inputs available with increased warming under SSP1-2.6, SSP2-4.5 and SSP5-8.5 (Table 1). We predict that organic C will be lost from soil in the

coastal temperate region at a decreasing rate between now and 2100, with the most significant losses before 2050 (Fig. 2h). The average loss of organic C relative to the baseline will be  $1.76 (\pm 1.19) \text{ t ha}^{-1}$  by 2020–2045 and  $4.67 (\pm 5.17) \text{ t ha}^{-1}$  by 2070–2100 under SSP1-2.6 (Table 1). MAOC and POC will be lost at similar rates between 2020 and 2045, but subsequently, MAOC will be lost more slowly than POC (Fig. 2h).

### Mapping the change

To represent the significant spatial and temporal variation in the change of TOC, POC and MAOC stocks throughout Australia, for each of the three SSPs, we mapped the predicted median change over 25-year periods from 2020–2045, 2045–2070 and 2070–2100 (see “Methods”) (Fig. 4). The spatial models were unbiased (mean deviations  $\approx 0$ ) and  $R^2$  values ranged between 0.73 and 0.92.

Under SSP1-2.6, relative to the baseline, we predict losses of organic C in the northernmost rangelands, and the losses will extend towards the south and west increasingly by 2045–2070 and 2070–2100 (Fig. 4a). MAOC will be lost in larger proportions than POC, and locally, in the southern rangelands, POC will increase somewhat (Fig. 4), possibly due to variable increases in precipitation. However, these small gains will not compensate for the loss of soil organic C in the rangelands. Under SSP2-4.5 and SSP5-8.5, there will be no regional gains in organic C, and the spatial patterns of the changes are similar, but the loss is more significant in 2070–2100 (Fig. 4b, c). Under SSP1-2.6, in 2020–2045, the median loss of organic C equates to  $0.293 (\pm 0.280) \text{ Gt}$ ,  $0.805 (\pm 1.033) \text{ Gt}$  in 2045–2070 and  $1.239 (\pm 1.784) \text{ Gt}$  in 2070–2100 (Fig. 4d). The loss is more significant under the SSP2-4.5 and SSP5-8.5 scenarios (Fig. 4e, f).

In the cropping region, dryland arable farming and modified pastures dominate. The simulations under all three SSPs predict that the soil will gain C but decreasingly with increased warming under SSP1-2.6 to SSP2-4.5 and SSP5-8.5, respectively. For SSP2-4.5 and SSP5-8.5, by 2070–2100, the maps show losses in the western extent of the eastern cropping region (Fig. 4b, c). However, these losses are offset by the gains in C elsewhere.

Under the more sustainable SSP1-2.6 scenario, the C gain in the period 2020–2045 is mainly in POC, but in time, by 2045–2070 and 2070–2100, the contribution from MAOC also increases as it is accrued (Fig. 4a). Under current management practices, soil used for cropping (and modified

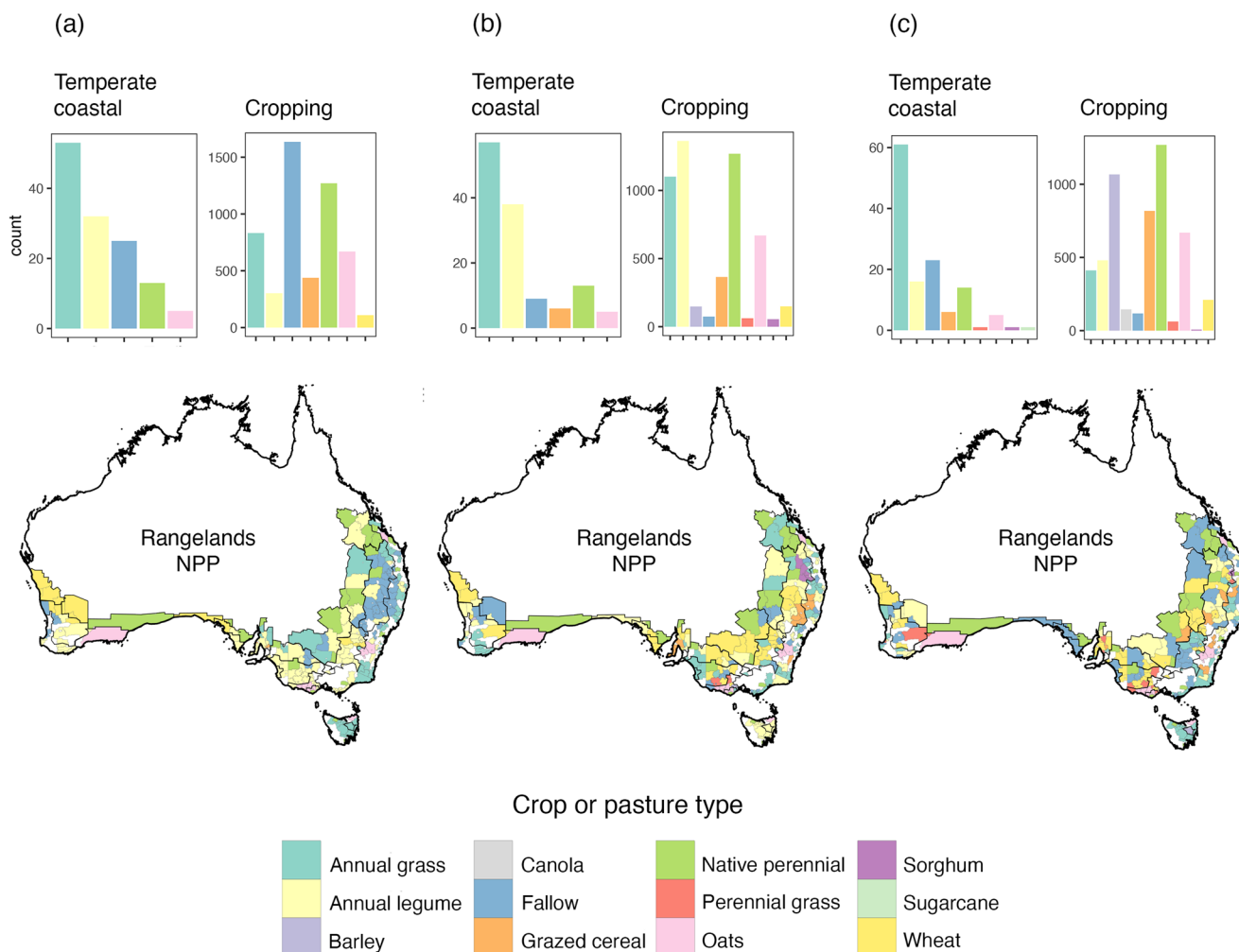


**Fig. 3 | Allocation of agricultural activities for deriving carbon (C) inputs.** In cropping and coastal temperate regions, which include areas of modified pastures, allocation occurred at a Statistical Area Level 2 (SA2). For carbon inputs in the

rangelands, we adjusted the monthly C inputs at the baseline with the annual rate of change in net primary productivity (NPP) from the ESMs. See “Methods” for details.

grazing) is a C sink, with predicted increases in total organic C under SSP1-2.6 of  $0.941 (\pm 0.509)$  Gt in 2020–2045,  $1.362 (\pm 0.901)$  Gt in 2045–2070 and  $1.579 (\pm 1.192)$  Gt by 2070–2100 (Fig. 4d). Under SSP2-4.5 and SSP5-8.5 the gains are smaller and by 2070–2100 under SSP5-8.5 it is  $0.880 (\pm 1.625)$  Gt (Fig. 4e, f). The wet coastal temperate regions support several forms of land use, from intensive farming and animal grazing mainly on modified pastures to temperate forests with the largest C stocks per unit area in Australia<sup>11</sup>. The predicted spatial pattern of the change in C shows increases in southeastern Australia, but losses predominate elsewhere from 2020–2045 to 2070–2100 and under the three SSPs (Fig. 4). The predicted change in MAOC and POC is similar in 2030 and 2050, but by 2100, the loss of MAOC is greater under all three scenarios (Fig. 4). The loss of organic C in coastal temperate regions is expected to increase from  $0.083 (\pm 0.182)$  Gt in 2020–2045 under SSP1-2.6 to  $0.254 (\pm 0.374)$  Gt in 2070–2100 under SSP5-8.5 (Fig. 4d–f).

### Magnitude of the future changes

In the 25 years between 2020 and 2045, we predict the median relative rate of soil organic C loss in Australia under the sustainable scenario, SSP1-2.6, to be  $0.0137 (\pm 0.0774)$  t ha<sup>-1</sup> year<sup>-1</sup> (Table 2). With a warmer climate under the middle of the road scenario, SSP2-4.5, the losses are larger, ranging from  $0.0228 (\pm 0.0871)$  t ha<sup>-1</sup> year<sup>-1</sup> in 2020–2045 and  $0.0343 (\pm 0.0602)$  t ha<sup>-1</sup> year<sup>-1</sup> in 2070–2100. Under SSP5-8.5 the loss is largest between  $0.070 (\pm 0.0861)$  t ha<sup>-1</sup>

year<sup>-1</sup> in 2020–2045 and  $0.0466 (\pm 0.0805)$  t ha<sup>-1</sup> year<sup>-1</sup> in 2070–2100 (Table 2).

In the rangelands, the predicted rates of C loss between 2020 and 2045 are similar for all three SSPs and range between  $0.0450 (\pm 0.0397)$  t ha<sup>-1</sup> year<sup>-1</sup> under SSP1-2.6 and  $0.0499 (\pm 0.0279)$  t ha<sup>-1</sup> year<sup>-1</sup> under SSP5-8.5. The rates of change between 2045 and 2070 and 2070–2100 increase somewhat but remain of similar magnitude with increased warming under the different emissions scenarios (Table 2).

In the cropping region, under the simulated activities (Fig. 3; see “Methods”) we predict a median annual sequestration of C in 2020–2045 of  $0.1947 (\pm 0.1682)$  t ha<sup>-1</sup> year<sup>-1</sup> for SSP1-2.6,  $0.0950 (\pm 0.1429)$  t ha<sup>-1</sup> year<sup>-1</sup> for SSP2-4.5 and  $0.1249 (\pm 0.1982)$  t ha<sup>-1</sup> year<sup>-1</sup> for SSP5-8.5 (Table 2). These values are within the range of sequestration rates of 0.1 to 0.4 t ha<sup>-1</sup> year<sup>-1</sup> reported in the literature for practices including stubble retention, reduced tillage and crop rotation<sup>28–30</sup>. In part, the predicted gains can be attributed to increases in C as the simulated agricultural management effectively counteracted the effect of a warming climate. Between 2045 and 2070, the sequestration rates decrease under the sustainable and middle-of-the-road scenarios, and with more severe warming under SSP5-8.5 C is lost at  $0.0302 (\pm 0.2192)$  t ha<sup>-1</sup> year<sup>-1</sup>. Between 2070 and 2100, the C sequestration rates decrease to  $0.0314 (\pm 0.1675)$  t ha<sup>-1</sup> year<sup>-1</sup> under SSP1-2.6 and with SSP2-4.5 and SSP5-8.5 we predict C losses at a rate of  $-0.0171 (\pm 0.1222)$  t ha<sup>-1</sup> year<sup>-1</sup> and  $-0.0663 (\pm 0.0983)$  t ha<sup>-1</sup> year<sup>-1</sup>, respectively (Table 2).

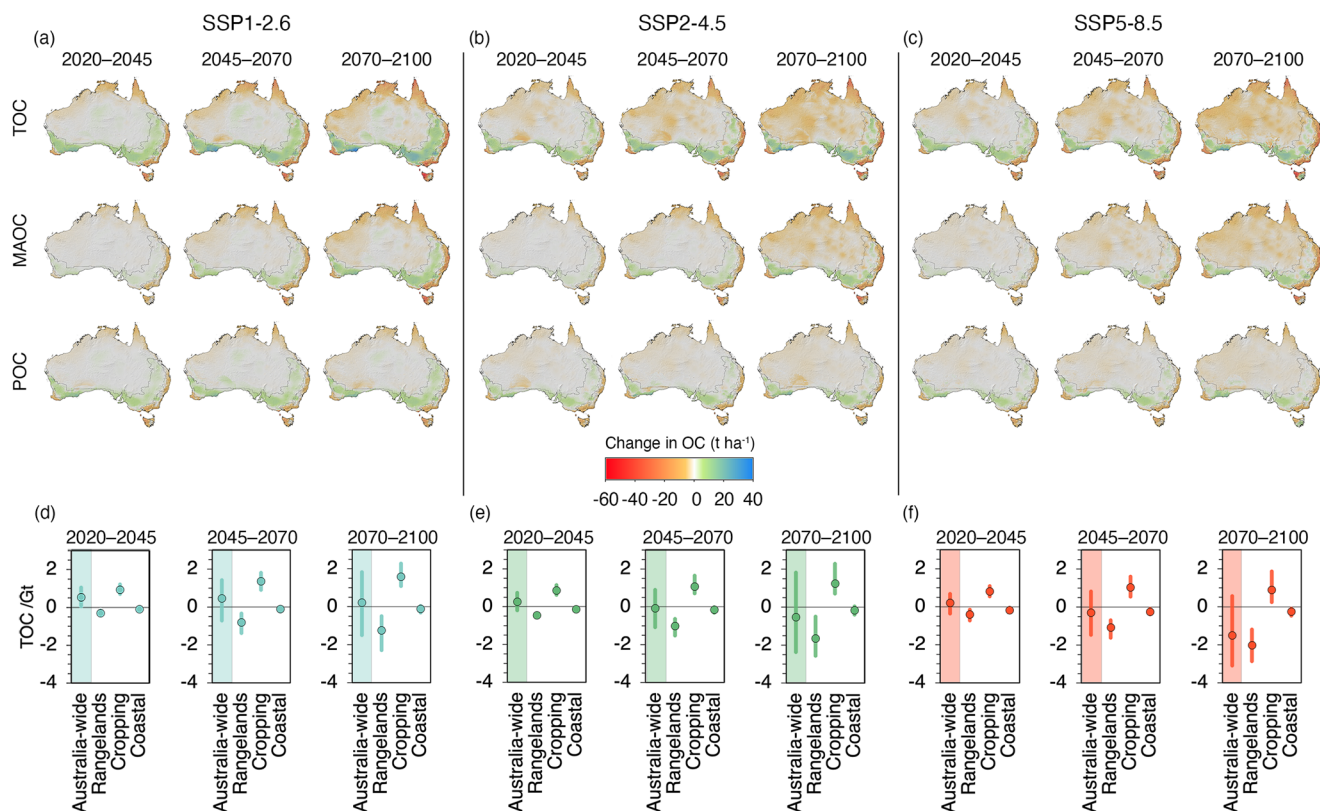


**Fig. 4 | The change in soil organic carbon (C) in Australia. a–c** Maps of the change in total (TOC), mineral-associated (MAOC) and particular (POC) organic carbon in Australia between the 1990–2010 baseline and 2020–2045, 2045–2070 and 2070–2100 ( $t\ ha^{-1}$ ), for the three shared socio-economic pathways (SSP) and six

climate models (Table 3). **d–f** Median total change reported in gigatonnes (Gt) for the predictions over all of Australia, the rangelands, the cropping and the coastal temperate regions. The error bars represent the interdecile range.

**Table 2 | Predicted median rates of change in total soil organic carbon (TOC) for periods 2020–2045, 2045–2070 and 2070–2100, in tonnes per hectare per year**

Scenario	TOC change / $t\ ha^{-1}\ year^{-1}$		
	SSP1-2.6	SSP2-4.5	SSP5-8.5
Year	Australia-wide		
2020–2045	– 0.0137 (0.0774)	– 0.0228 (0.0871)	– 0.0770 (0.0861)
2045–2070	– 0.0101 (0.0828)	– 0.0106 (0.0617)	– 0.0436 (0.0722)
2070–2100	– 0.0125 (0.0413)	– 0.0343 (0.0602)	– 0.0466 (0.0805)
	Rangelands		
2020–2045	– 0.0450 (0.0397)	– 0.0499 (0.0279)	– 0.0442 (0.0366)
2045–2070	– 0.0253 (0.0612)	– 0.0339 (0.0465)	– 0.0526 (0.0458)
2070–2100	– 0.0297 (0.0277)	– 0.0358 (0.0393)	– 0.0522 (0.0603)
	Cropland		
2020–2045	0.1947 (0.1682)	0.0950 (0.1429)	0.1640 (0.1982)
2045–2070	0.0949 (0.1671)	0.0939 (0.1589)	– 0.0302 (0.2192)
2070–2100	0.0314 (0.1675)	– 0.0171 (0.1222)	– 0.0663 (0.0983)
	Coastal		
2020–2045	– 0.0925 (0.0933)	– 0.1106 (0.0845)	– 0.1366 (0.0953)
2045–2070	– 0.0361 (0.0752)	– 0.0664 (0.0920)	– 0.0851 (0.1007)
2070–2100	– 0.0320 (0.0616)	– 0.0287 (0.0458)	– 0.0363 (0.0609)

Values in brackets represent the interdecile ranges.

In the coastal temperate region, the predicted rate of change between 2020 and 2045 is  $-0.0925(\pm 0.0933)\ t\ ha^{-1}\ year^{-1}$  under SSP1-2.6, increasing to  $-0.1366(\pm 0.0953)\ t\ ha^{-1}\ year^{-1}$  under SSP5-5.85 (Table 2). The rates at which C is lost decrease in 2045–2070 and 2070–2100, but increase with increasing warming (Table 2).

### Discussion

Under the prevailing (middle-of-the-road) socioeconomic scenario of SSP2-4.5, characterized by modest shifts from historical patterns and a future where efforts to reduce emissions are insufficient to limit global warming to that required for a more sustainable and climate-resilient future, our predictions suggest that Australian soil will act as a net emitter of C, in addition to CO<sub>2</sub> emissions predicted from all sectors of the Australian economy. In the 25 years between 2020 and 2045, we predict median emissions from soil to reach  $0.064(\pm 0.197)\ Gt\ CO_2-e\ year^{-1}$  (CO<sub>2</sub>-equivalent) (Fig. 5). By 2045–2070, this trajectory predicts emissions of  $0.030(\pm 0.320)\ Gt\ CO_2-e\ year^{-1}$  and  $0.097(\pm 0.176)\ Gt\ CO_2-e\ year^{-1}$  by 2070–2100 (Fig. 5). The emissions during 2020–2045 are equivalent to 14% of Australia’s total 2022 emissions of 0.464 Gt CO<sub>2</sub>-e from all sectors of the economy, 82% of emissions from agriculture (0.078 Gt CO<sub>2</sub>-e), and 18% of the forecasted total emissions of 0.354 Gt CO<sub>2</sub>-e in 2030<sup>31</sup>.

Scenario SSP5-8.5 may seem improbable<sup>32</sup>, but we included it because it matches the increases in emissions and global temperatures over the past two decades<sup>33</sup>. It is an upper limit in our modeling, illustrating the potential consequences if those trends continue unabated. Under this scenario, soil emissions in 2020–2045 will be greater than those of middle-of-the-road or more sustainable scenarios, but predictions are also more uncertain (Fig. 5). By 2045–2070, under this trajectory, Australian soil will emit  $0.123(\pm 0.148)$

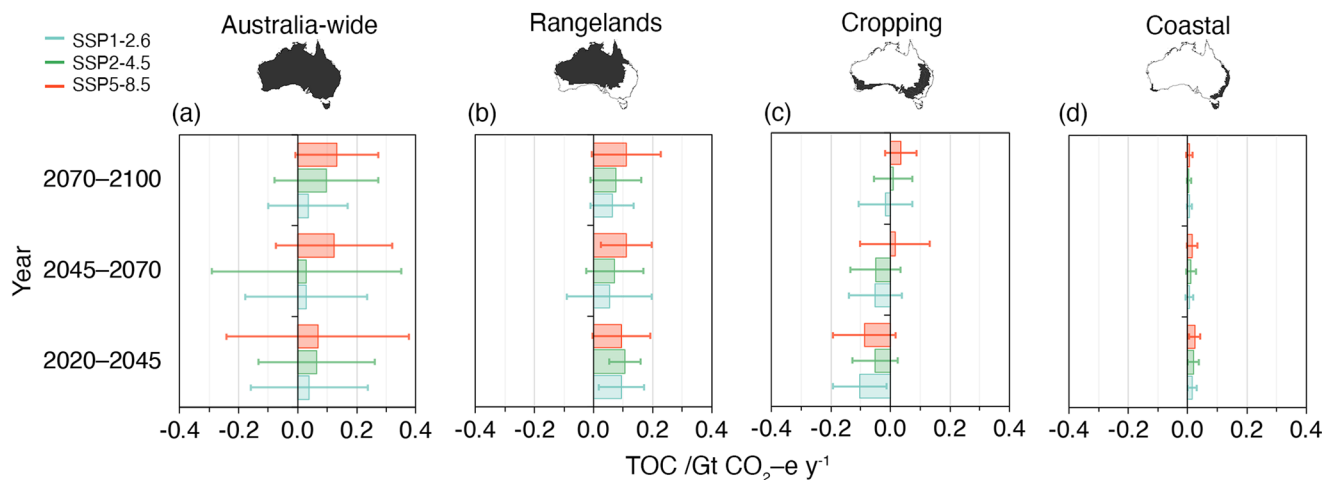


**Fig. 5** | Median relative change in total organic carbon (TOC) during 25-year periods. **a** Over all of Australia, **b** the rangelands, **c** cropping regions and **d** coastal temperate regions, for each of the three shared socioeconomic pathways, SSP1-2.6, SSP1-2-4.5, SSP1-5-8.5. Error bars represent the interdecile range.

Gt CO<sub>2</sub>-e year<sup>-1</sup>, which is equivalent to 35% of Australia’s total projected emissions in 2030<sup>31</sup>. In 2070–2100, we predict emissions from soil will increase further (Fig. 5).

Under SSP1-2.6, which imagines a socioeconomic shift toward sustainability, we predict emissions from soil to be smaller than the other scenarios, reaching 0.039 (± 0.198) Gt CO<sub>2</sub>-e year<sup>-1</sup> in the 25 years between 2020–2045 (Fig. 5). These are the smallest predicted emissions from Australian soil and are equivalent to 8.3% of Australia’s total emissions for 2022, 49% of agricultural emissions, and 11% of the total emissions forecast for 2030<sup>31</sup>. This trajectory predicts emissions of 0.029 (± 0.207) Gt CO<sub>2</sub>-e year<sup>-1</sup> by 2045–2070 and 0.035 (± 0.135) Gt CO<sub>2</sub>-e year<sup>-1</sup> by 2070–2100 (Fig. 5).

Uncertainty in model predictions of future soil C dynamics is well documented, and our understanding of the sources of this uncertainty is evolving<sup>34</sup>. Our study strived to reduce parameter and input data uncertainty in the simulations by calibrating Roth C to Australian conditions<sup>18</sup>, parameterizing the main conceptual pools in Roth C, the RPM, HUM, and IOM, with measured POC, MAOC, and pyrogenic organic C fractions, respectively<sup>35</sup>, using region-specific approaches to derive future C inputs in cropping, coastal and rangeland areas with different possible crop types, NPP, and accounting for the CO<sub>2</sub> fertilization effect, using a selection of six ESMS from the CMIP6, correcting for bias in the future climate data, and propagating the uncertainties from the ESMS and C inputs through the predictions of future soil C stocks. We do not account for structural model uncertainty because models with relatively simple structures (such as Roth C) are known to produce predictions of soil C dynamics with smaller uncertainty over larger scales, compared to more complex models, which produce much more significant uncertainties in response to climate change<sup>36</sup>.

As part of international efforts to mitigate climate change, the Australian government’s revised Nationally Determined Contribution (NDC) aims for a 43% emissions reduction by 2030 and ‘net zero’ by 2050<sup>31</sup>, thus achieving its commitment to the Paris Agreement and keeping 1.5°C within reach. Australia’s Long-Term Emissions Reduction Plan<sup>37</sup> identifies soil C as a priority low-emissions technology, proposing that improved management of one-quarter of Australia’s crop and grazing soil could sequester 0.035–0.090 Gt CO<sub>2</sub>-e year<sup>-1</sup>, or as much as 0.103 Gt CO<sub>2</sub>-e year<sup>-1</sup> in areas with more rain<sup>37</sup>. However, our findings suggest that those estimates are overly optimistic; we predict more modest gains under current practice. Under SSP2-4.5, in all of Australia’s cropping regions (including modified grazing) over the 25 years from 2020 to 2045, we predict median sequestration rates of 0.051 (± 0.076) Gt CO<sub>2</sub>-e year<sup>-1</sup>, ranging from 0.104 (± 0.090) Gt CO<sub>2</sub>-e year<sup>-1</sup> under SSP1-2.6 to 0.088 (± 0.106) Gt CO<sub>2</sub>-e year<sup>-1</sup> under SSP5-8.5. The predicted gains in cropping regions decrease to roughly half that in 2045–2070. Under SSP2-4.5 and SSP5-8.5, the gains are

smaller, and by 2070–2100 under SSP2-4.5 and 2045–2100 under SSP5-8.5, Australian soil is a net C emitter of up to 0.036 (± 0.052) Gt CO<sub>2</sub>-e year<sup>-1</sup> (Fig. 5).

Our results show that warmer and drier conditions will lead to more significant C loss in the rangelands than elsewhere in Australia. Under SSP1-2.6, in the 25 years between 2020–2045, the net loss of soil organic C in the rangelands corresponds to emissions of 0.095 (± 0.077) Gt CO<sub>2</sub>-e year<sup>-1</sup>. By 2045–2070 and 2070–2100, the predicted emissions decrease slightly as a more favorable climate stimulates plant growth and increases in soil C in the central and southern rangelands (Fig. 4). Emissions are greater under the SSP2-4.5 and SSP5-8.5 scenarios (Fig. 5). The rangelands of Australia are diverse. They sustain biodiversity that has been little altered since the advent of European settlement, indigenous cultures, and pastoral and mining industries. The risks and threats to rangeland ecosystems from climate change are global and systemic. Any change to the use or management must recognize that rangelands are also complex and adaptive ecosystems where organic C can cycle through phases of accumulation, conservation, and loss after disturbance from, for example, clearing, overgrazing, fire, drought or flood<sup>25</sup>.

Significantly, the soil organic C losses from the rangelands and the coastal temperate region, which occupy approximately 82% of the country, are not offset by the predicted gains of soil C under cropping (Fig. 4). Rangeland soils have potential for C sequestration<sup>38</sup>, but much of the region has a dry and variable climate; its productive capacity is small because vegetative cover is sparse, and it suffers from alterations that result in livestock grazing, frequent fires, weed infestations and grazing by feral animals<sup>25</sup>. Overcoming these to sequester additional C will be difficult, but rangeland soil could capture at least some of that potential by improving grazing management, enacting cultural burning practices, and regenerating biodiverse, endemic native plant communities. With more organic C, soils could absorb and store more water, reduce erosion, enhance biodiversity and lead to more stable ecosystems<sup>39</sup>.

The predicted net losses of organic C from soil will significantly affect Australia’s ability to achieve its GHG emissions reduction target. If Australia could shift from its current behavior towards a more sustainable pathway, it would be better able to meet its target. For this shift to occur, however, it must embrace existing GHG removal technologies and develop new large-scale solutions to achieve sustainability. Australia would have to build on the potential of agriculture to sequester C in the soil and to improve soil conservation in the rangelands. It could do so by continuing to support and develop scientifically sound carbon crediting initiatives (such as the Australian Carbon Credit Unit (ACCU) scheme) and Nature Positive plans, which provide economic incentives for farmers and land managers to sequester C and conserve biodiversity on their land actively. Although not a

panacea, such nature-based schemes must be integral to government policies. By doing so, policymakers can encourage sustainable practices while bolstering the agricultural and environmental sectors' roles in achieving national emission reduction targets.

Our findings present decision-makers and researchers with information on the significance of soil organic C for Australia's greenhouse gas inventory. Addressing the vulnerability of soil C stocks in the rangelands and coastal temperate regions and continuing to harness the potential for sequestration in cropping areas must become integral components of Australia's emissions reduction strategies towards a sustainable environmental future. Climate change is a difficult problem that requires a global, multifaceted, and interdisciplinary approach to address it effectively. Australia and other countries must consider the soil and enact effective action and collaborations with researchers and stakeholders to pave the way for sustainable climate change mitigation, environmental preservation and conservation.

## Methods

### Model description

Roth C models the processes by which organic C changes in the soil. It has a monthly time step and four active pools: decomposable plant material (DPM), resistant plant material (RPM), microbial biomass (BIO) and humified organic matter (HUM), plus a pool of inert organic matter (IOM). We used version 26.3 of the model. The model was calibrated for a range of Australian agricultural systems<sup>40</sup> and used for the soil C component of the Full Carbon Accounting Model (FullCAM) in the Australian National Greenhouse Gas Inventory<sup>17</sup>. The decomposition rate constants for the DPM, RPM, BIO, and HUM pools are 10, 0.3, 0.15 and 0.02 year<sup>-1</sup>, respectively<sup>40</sup>. The active pools decompose following first-order kinetics. They are assumed to increase with increasing air temperature but are reduced by soil water deficit and vegetated soil cover. The soil cover factor is set to 1.0 for bare soil and 0.6 to slow organic matter decomposition when soil is vegetated. Incoming C from plant residues or exogenous organic matter (e.g., manure) is split between DPM and RPM, decomposed to BIO and HUM and lost as CO<sub>2</sub>. The conceptual pools of RPM, HUM and IOM in the original model were replaced with the measurements of particulate (POC), mineral-associated (MAOC) and resistant organic C (PyC) fractions, respectively<sup>40,41</sup>.

### Input data for the simulations

We used a subset of the soil data on the POC, MAOC and PyC fractions in the 0–30 cm layer at 4045 sites across Australia, which we compiled in previous studies<sup>18,35,42</sup>. The samples represent all Australian soil classification orders<sup>43</sup>, except for Anthrospols, all land use types, and all states and territories of Australia. Other soil attributes needed for the simulations include clay content (%), bulk density (g cm<sup>-3</sup>) and available water capacity (AWC) (mm m<sup>-1</sup>), and we sourced these from<sup>42</sup>.

Data on historical and current air temperature, precipitation and pan evaporation were obtained from the SILO database of Australian climate data<sup>44</sup>. We estimated pan-evaporation by dividing the evaporation rates from the ESMs (see below) by site-specific pan coefficients that we acquired from the SILO<sup>44</sup> data for the years 1991 to 2018.

Data on land use at the national (1:2 500 000) scale (NLUM) were obtained from the Australian Bureau of Agricultural and Resource Economics and Sciences<sup>45</sup>. The NLUM data include information on detailed land uses. We re-classified the land use at each site into four broad land uses: arable cropping, modified grazing, native grazing, and areas for nature conservation, including for indigenous and other minimal uses. The model requires C inputs. We estimated these monthly using the four land use classes, vegetation type and management regimes, and a crop model, as described in<sup>18</sup> and briefly described next.

### Baseline simulations of soil organic C

Lee et al.<sup>18</sup> provide the details on the baseline simulations. In the following, we summarize the main points relevant to this study. We selected the

1991–2010 to represent the baseline and as the benchmark for the (future) simulations. The model was initialized with the measured POC, MAOC and PyC fractions and clay content (see above). We extracted daily weather data for the baseline period from SILO and aggregated them to monthly total precipitation, pan evaporation, and average air temperature. We estimated monthly C inputs as follows. Under arable cropping, we assumed that crops were grown in rotations. To determine the rotations during the baseline period, we used data on agricultural activities and crop types<sup>46</sup> at the Statistical Area Level 2 (SA2), which are functional areas that represent socially and economically coherent communities<sup>47</sup>. For modified grazing sites, we used only a single annual or perennial grass species<sup>46</sup>, while for native grazing sites, we used a perennial native grass. For the sites under nature conservation, we assumed small but consistent C inputs from plant residues only<sup>48</sup> and set the C inputs at a constant value of 0.049 t ha<sup>-1</sup> month<sup>-1</sup>.

To simulate plant growth, we used a crop model by<sup>49</sup> that uses the amount of water available to the plant (derived from the AWC) to derive a potential dry matter increment that is water-limited (WLDM). We calculated the WLDM from the fraction of evapotranspiration that is transpired, the fraction of deep water drainage that occurs during the fallow period, and the transpiration efficiency of the crop or pasture<sup>18</sup>. Evapotranspiration and deep drainage were derived by a soil water balance with pan evaporation, rainfall, clay content, bulk density, and specific crop parameters<sup>49</sup>. Thus, the model calculates dry matter production incrementally to produce the accumulated dry matter in a season. For perennial plant growth, the model calculates dry matter production over the seasons. The model estimates root biomass using a fixed root-to-shoot ratio of 0.3. For both modified and native pastures, we assumed grazing to occur if the grass accumulated 1.2 t ha<sup>-1</sup> of shoot dry matter, with no grazing effect on its growth. We also assumed that grazing animals consumed 50% of daily shoot growth, returned 50% of the consumption to the soil as dung and shed 50% of daily root growth. When the available soil water fell to <15% of water holding capacity, we assumed that 1% and 0.5% of the shoot and root dry matter died daily. The C content of above-ground and below-ground residues was 42% by mass, which is the value used in the FullCAM<sup>17</sup>.

We adjusted the estimated initial C inputs iteratively to fit the simulated C pools to the measured TOC, POC, and MAOC, assuming long-term (100-year) steady-state equilibrium and selected the DPM/RPM ratio that produced the smallest deviation between the measured and simulated stock of TOC. We repeated the weather data under the same average management regimes to attain this condition in the simulations. Therefore, we optimised the amount, timing, and quality of C inputs at each site to maintain current soil organic C stocks.

### Future simulations

To simulate soil organic C between 2010 and 2100, we assumed constant land management so that the predicted change would depend only on changes in climate. Thus, we used climate projections from the different ESMs for the simulation, considering three shared socio-economic scenarios (SSPs) and with C inputs derived from agricultural activities in rotations and simulated NPP.

**Climate data and NPP.** We used monthly climate data (2-degree resolution) for the years 2000 to 2100 from six ESMs from the Coupled Model Inter-comparison Project Phase 6 (CMIP6) (Table 3).

We used projected NPP from the ESMs and NPP from a MODIS NPP product (MOD17A3H) for 2002–2016<sup>50</sup> to estimate the annual rate of change in NPP for the 2010 to 2100 period. In this way, our simulations could account for the CO<sub>2</sub> fertilization effect and the increase in transpiration efficiency<sup>51</sup>. Before using the climate projections, we removed bias from the future monthly data with the multivariate bias correction algorithm, which uses a multivariate generalization of the quantile regression method to correct for biases in climate variables from ESMs<sup>52</sup>. We used the reference period between 1970 and 2010 for the corrections and implemented the techniques with the R package MBC<sup>53</sup>.

**Table 3 | Earth system models (ESM) and their climate projections used in the simulations**

Earth system model	Description	Land component	Reference
ACCESS-ESM1.5	Australian Community Climate and Earth System Simulator, version 1.5	Community Atmosphere Biosphere Land Exchange (CABLE)	60
CESM2	Community Earth System Model version 2	Community Land Model (CLM)	61
CNRM-ESM2-1	Center National de Recherches Météorologiques Earth System Model, version 2.	Interaction Soil-Biosphere-Atmosphere-CNRM Total Runoff Integrating Pathways coupled system	62
IPSL-CM6A-LR	L'Institut Pierre-Simon Laplace, Coupled Model, low resolution version 6	Organizing C and Hydrology in Dynamic Ecosystems (ORCHIDEE)	63
MIROC-ES2L	Model for Interdisciplinary Research on Climate Earth System version 2, for Long-term simulations	Spatially Explicit Individual-Based Dynamic Global Vegetation Model (SEIB-DGVM)	64
NorESM2-LM	Norwegian Earth System Model, version 2, low-medium resolution	Community Land Model (CLM)	65

The climate data are available at the Earth System Grid Federation portal: <https://esgf-node.llnl.gov/projects/cmip6/>.

**Future carbon inputs.** To simulate future C inputs under cropping and coastal regions, we used historical agricultural activity data and crop type in each SA2 region for 1970–2015<sup>46</sup>. Under cropping, we again assumed that crops were grown in rotations, while for coastal areas, we assumed the growth of a single grass species (Fig. 3). To quantify the organic C response of soil to future climate while considering possible crop and pasture rotations, we identified the three most representative crop or grass species at each site in an SA2 region. We ran the crop model with the most representative crop type and used the six climate models per SSP scenario to derive the C inputs (see above) for the Roth C simulations. Then, we repeated for the second and third most representative crop types. For modified grazing sites, which also represent coastal temperate regions, we used only one annual or perennial grass species in the rotation (see above).

For areas under native grazing and under nature conservation, which represent the Australian rangelands, we assumed that future changes in soil organic C would be driven mainly by changes in future NPP and climate. Thus, to account for the amount and timing of C inputs in 2010–2100, we adjusted the monthly C inputs with the annual rate of change in NPP (see above) and combined the results. In this way, we could account for the fertilization effect of CO<sub>2</sub> and increases in transpiration efficiency<sup>51</sup>.

### Analyses

We addressed uncertainty in model inputs due to different climate change predictions with the several ESMs for each SSP. We calculated the median annual TOC, POC, and MAOC from estimates with each ESM and SSP across the sites from 2010 to 2100. We used an 11-year moving average to focus on longer-term trends rather than year-to-year fluctuations in the data. We calculated changes in temperature, precipitation, and organic C relative to the 1990–2010 baseline for four distinct periods: 2010–2020 representing the recent past, 2020–2045 representing the near future, 2045–2070 representing the mid-future and 2070–2100 the far-future. We report results in tonnes C per hectare (t ha<sup>-1</sup>) and gigatonnes C, calculated as  $GtC = C(t\ ha^{-1}) \times Area$  (hectares)  $\div 10^9$ . We also report the relative annual change in soil organic C for 2020–2045, 2045–2070 and 2070–2100 in tonnes of C per hectare per year (t ha<sup>-1</sup> year<sup>-1</sup>) and in gigatonnes CO<sub>2</sub>-equivalents per year, calculated by  $Gt\ CO_2 - e\ year^{-1} = C\ change(t\ ha^{-1}\ year^{-1}) \times Area$  (hectares)  $\times 3.67 \div 10^9$ , where 3.67 is the molecular weight ratio of CO<sub>2</sub> (44) to C (12). We chose 25-years for the near- and mid-futures as it corresponds to the minimum permanence period that soil C must be stored in sequestration projects under the Australian Carbon Credit Units (ACCU) scheme.

The uncertainty around the climate projections, soil organic C stocks, and C inputs were calculated as the difference between the first and the ninth deciles (10% and 90%), i.e. the interdecile range.

### Mapping

We mapped the 4045 predictions of TOC, POC and MAOC for each of the three SSPs using data representing 25-year periods from 2020–2045, 2045–2070 and 2070–2100 by interpolation with punctual kriging with external drift (KED)<sup>54</sup>, as follows. We used cubist<sup>42,55,56</sup> to model the response variables at the 4045 sites as functions of the spatially explicit forcings for the respective decade and SSP and a set of static covariates representing soil and landscape attributes. All covariates were resampled to a 1 km pixel resolution by bilinear interpolation. The climate and vegetation forcing used were the average of the mean annual temperature (MAT), mean annual precipitation (MAP), mean pan evaporation, and NPP from the six ESMs (Table 3). We also derived the Prescott index<sup>57</sup> for each year and SSP combination from those data. The static covariates were the digital elevation model (DEM), slope, topographic wetness index (TWI); mineralogy, represented by the gamma radiometric total dose and potassium, and the clay minerals kaolinite, illite and smectite<sup>58</sup>. We then used the respective models to predict the TOC, POC, and MAOC stock at each future period and for each SSP elsewhere across Australia. The cubist maps of the response variables were the external drift covariates in the KED of the TOC, POC and MAOC stocks. The advantages of this approach are that the modeling with cubist to derive the covariates helps capture any non-linear responses in the modeling, and the KED provides the uncertainties of the mapping<sup>59</sup>. We validated the models with a 10-fold cross validation and, to assess them, recorded the coefficient of determination (R<sup>2</sup>). The 1 km resolution digital maps helped to identify the regional spatial and temporal variability of predicted future C stocks and composition in Australia and their susceptibility to change.

### Data availability

The soil dataset is available from Zenodo (<https://doi.org/10.5281/zenodo.10783970>). The climate data are available at the Earth System Grid Federation portal (<https://esgf-node.llnl.gov/projects/cmip6/>). Other spatial datasets are available from the Terrestrial Ecosystem Research Network (TERN) data portal (<https://portal.tern.org.au>). The Roth-C model is available from Rothamsted Research (<https://www.rothamsted.ac.uk/rothamsted-carbon-model-rothc>) and in R via the *SoilR* library (<https://cran.r-project.org/web/packages/SoilR/index.html>). Our implementation and the code for processing the input datasets and for collating the outputs from the simulations is available from the corresponding author on request.

### Code availability

The soil dataset is available from Zenodo (<https://doi.org/10.5281/zenodo.10783970>). The climate data are available at the Earth System Grid Federation portal (<https://esgf-node.llnl.gov/projects/cmip6/>). Other spatial datasets are available from the Terrestrial Ecosystem Research Network (TERN) data portal (<https://portal.tern.org.au>). The Roth-C model is available from Rothamsted Research (<https://www.rothamsted.ac.uk/rothamsted-carbon-model-rothc>) and in R via the *SoilR* library (<https://>

[cran.r-project.org/web/packages/SoilR/index.html](https://cran.r-project.org/web/packages/SoilR/index.html)). Our implementation and the code for processing the input datasets and for collating the outputs from the simulations is available from the corresponding author on reasonable request.

Received: 21 September 2023; Accepted: 6 March 2024;  
Published online: 26 March 2024

## References

- Batjes, N. H. Total carbon and nitrogen in the soils of the world. *Eur. J. Soil Sci.* **47**, 151–163 (1996).
- Le Quéré, C. et al. Global carbon budget 2018. *Earth Syst. Sci. Data* **10**, 2141–2194 (2018).
- Friedlingstein, P. et al. Global carbon budget 2022. *Earth Syst. Sci. Data* **14**, 4811–4900 (2022).
- Rumpel, C. et al. Put more carbon in soils to meet Paris climate pledges. *Nat.* **564**, 32–34 (2018).
- Adler, C. et al. Cross-chapter paper 5: Mountain. In: H. O. Pörtner et al. (Eds.) *Climate Change 2022: Impacts, Adaptation and Vulnerability. Contribution of Working Group II to the Sixth Assessment Report of the Intergovernmental Panel on Climate Change*. Cambridge University Press, Cambridge, UK and New York, NY, USA, pp. 2273–2318 (2022).
- Griscom, B. W. et al. Natural climate solutions. *Proc. Natl. Acad. Sci. USA* **114**, 11645–11650 (2017).
- Bossio, D. A. et al. The role of soil carbon in natural climate solutions. *Nat. Sustain.* **3**, 391–398 (2020).
- Arias, P.A. et al. Technical Summary. In: Masson-Delmotte, V. et al. (Eds.) *Climate Change 2021: The Physical Science Basis. Contribution of Working Group I to the Sixth Assessment Report of the Intergovernmental Panel on Climate Change*. Cambridge University Press, Cambridge, United Kingdom and New York, NY, USA, pp. 33–144 (2021).
- Canadell, J. G. et al. Multi-decadal increase of forest burned area in Australia is linked to climate change. *Nat. Commun.* **12**, 1–11 (2021).
- Byrne, B. et al. The carbon cycle of southeast Australia during 2019–2020: Drought, fires, and subsequent recovery. *AGU adv.* **2**, 1–20 (2021).
- Walden, L. et al. Multi-scale mapping of Australia’s terrestrial and blue carbon stocks and their continental and bioregional drivers. *Commun. Earth Environ.* **4**, 1–12 (2023).
- Viscarra Rossel, R. A., Webster, R., Bui, E. N. & Baldock, J. A. Baseline map of organic carbon in Australian soil to support national carbon accounting and monitoring under climate change. *Glob. Change Biol.* **20**, 2953–2970 (2014).
- Liao, Z. M., Van Dijk, A. I. J. M., He, B. B., Larraondo, P. R. & Scarth, P. F. Woody vegetation cover, height and biomass at 25-m resolution across Australia derived from multiple site, airborne and satellite observations. *Int. J. Appl. Earth Obs. Geoinf.* **93**, 1–12 (2020).
- Luo, Z. K., Wang, E. L. & Sun, O. J. Soil carbon change and its responses to agricultural practices in Australian agro-ecosystems: a review and synthesis. *Geoderma* **155**, 211–223 (2010).
- Sanderman, J., Hengl, T. & Fiske, G. J. Soil carbon debt of 12,000 years of human land use. *Proc. Natl. Acad. Sci. USA* **114**, 9575–9580 (2017).
- Coleman, K. & Jenkinson, D.S. RothC-26.3—a model for the turnover of carbon in soil. In: Powlson, D.S., Smith, P. & Smith, J.U. (Eds.) *Evaluation of soil organic matter models: using existing long-term datasets*. Nato ASI Subseries I, Volume 38. Springer, Berlin, pp. 237–246 (1996).
- Richards, G. & Evans, D. Development of a carbon accounting model (FullCAM Vers. 1.0) for the Australian continent. *Aust. For.* **67**, 277–283 (2004).
- Lee, J., Viscarra Rossel, R. A., Zhang, M. X., Luo, Z. K. & Wang, Y. P. Assessing the response of soil carbon in Australia to changing inputs and climate using a consistent modelling framework. *Biogeosciences* **18**, 5185–5202 (2021).
- Eyring, V. et al. Overview of the Coupled Model Intercomparison Project Phase 6 (CMIP6) experimental design and organization. *Geosci. Model Dev.* **9**, 1937–1958 (2016).
- Chen, D. et al. Framing, Context and Methods. In: Masson-Delmotte, V. et al. (Eds.) *Climate Change 2021: The Physical Science Basis. Contribution of Working Group I to the Sixth Assessment Report of the Intergovernmental Panel on Climate Change*. Cambridge University Press, Cambridge, United Kingdom and New York, NY, USA, pp. 147–286 (2021).
- O’Neill, B. C. et al. The roads ahead: Narratives for shared socioeconomic pathways describing world futures in the 21st century. *Glob. Environ. Change* **42**, 169–180 (2017).
- Meinshausen, M. et al. The shared socio-economic pathway (SSP) greenhouse gas concentrations and their extensions to 2500. *Geosci. Model Dev.* **13**, 3571–3605 (2020).
- Boone, R. B., Conant, R. T., Sircely, J., Thornton, P. K. & Herrero, M. Climate change impacts on selected global rangeland ecosystem services. *Glob. Change Biol.* **24**, 1382–1393 (2018).
- Poulter, B. et al. Contribution of semi-arid ecosystems to interannual variability of the global carbon cycle. *Nat.* **509**, 600–603 (2014).
- Foran, B. et al. Australian rangeland futures: time now for systemic responses to interconnected challenges. *Rangel. J.* **41**, 271–292 (2019).
- Unkovich, M., Baldock, J. & Marvanek, S. Which crops should be included in a carbon accounting system for Australian agriculture? *Crop Pasture Sci.* **60**, 617–626 (2009).
- Llewellyn, R. S., D’Emden, F. H. & Kuehne, G. Extensive use of no-tillage in grain growing regions of Australia. *Field Crops Res.* **132**, 204–212 (2012).
- Sanderman, J. & Baldock, J. A. Accounting for soil carbon sequestration in national inventories: a soil scientist’s perspective. *Environ. Res. Lett.* **5**, 1–6 (2010).
- Chan, K. Y. et al. Soil carbon dynamics under different cropping and pasture management in temperate Australia: Results of three long-term experiments. *Soil Res.* **49**, 320–328 (2011).
- Lam, S. K., Chen, D., Mosier, A. R. & Roush, R. The potential for carbon sequestration in Australian agricultural soils is technically and economically limited. *Sci. Rep.* **3**, 1–6 (2013).
- DCCEEW Department of Climate Change, Energy, the Environment and Water. National Inventory Report. Australian Government, Canberra. <https://www.dcceew.gov.au/climate-change/publications/national-inventory-report-2021> (2023).
- Hausfather, Z. & Peters, G. P. Emissions—the ‘business as usual’ story is misleading. *Nat.* **577**, 618–620 (2020).
- Schwalm, C. R., Glendon, S. & Duffy, P. B. RCP8.5 tracks cumulative CO<sub>2</sub> emissions. *Proc. Natl. Acad. Sci. USA* **117**, 19656–19657 (2020).
- Luo, Y. et al. Toward more realistic projections of soil carbon dynamics by Earth system models. *Global Biogeochem. Cycles* **300**, 40–56 (2016).
- Viscarra Rossel, R. A. et al. Continental-scale soil carbon composition and vulnerability modulated by regional environmental controls. *Nat. Geosci.* **12**, 547–552 (2019).
- Shi, Z., Crowell, S., Luo, Y. & Moore III, B. Model structures amplify uncertainty in predicted soil carbon responses to climate change. *Nat. Commun.* **9**, 1–11 (2018).
- DCCEEW Department of Climate Change, Energy, the Environment and Water. Australia’s long-term emissions reduction plan. Australian Government, Canberra. <https://www.dcceew.gov.au/sites/default/files/documents/australias-long-term-emissions-reduction-plan.pdf> (2021).
- Viscarra Rossel, R. A. et al. How much organic carbon could the soil store? The carbon sequestration potential of Australian soil. *Glob. Change Biol.* **30**, e17053 (2024).

39. White, R. E. The role of soil carbon sequestration as a climate change mitigation strategy: An Australian case study. *Soil Syst.* **6**, 46–59 (2022).
40. Skjemstad, J. O., Spouncer, L. R., Cowie, B. & Swift, R. S. Calibration of the Rothamsted organic carbon turnover model (RothC ver. 26.3), using measurable soil organic carbon pools. *Aust. J. Soil Res.* **42**, 79–88 (2004).
41. Baldock, J. A. et al. Quantifying the allocation of soil organic carbon to biologically significant fractions. *Soil Res.* **51**, 561–576 (2013).
42. Viscarra Rossel, R. A. et al. The Australian three-dimensional soil grid: Australia's contribution to the globalsoilmap project. *Soil Res.* **53**, 845–864 (2015).
43. Isbell, R. *The Australian Soil Classification*. CSIRO Publishing, Melbourne, Australia (2016).
44. Queensland Department of Environment and Science. SILO: Australian climate data from 1889 to the present. <https://www.longpaddock.qld.gov.au/silo/> (2021)
45. ABARES Australian Bureau of Agricultural and Resource Economics and Sciences. ABARES: Land use of Australia 2010–11. <https://www.agriculture.gov.au/abares/data> (2021).
46. Unkovich, M., Baldock, J. & Farquharson, R. *Development of comprehensive time-series datasets of crop and pasture type and management, for the Australian continent, relevant to the national greenhouse gas inventory carbon accounting procedures*. Technical Report, CSIRO, Australia (2017).
47. ABS, Australian Bureau of Statistics. ABS: Statistical area level 2 (SA2), statistical geography. Canberra. <https://www.abs.gov.au/websitedbs/D3310114.nsf/home/geography> (2016).
48. Wang, Y. P. & Barrett, D. J. Estimating regional terrestrial carbon fluxes for the Australian continent using a multiple-constraint approach sensed data and ecological observations of net primary production. *Tellus B Chem. Phys. Meteorol.* **55**, 270–289 (2003).
49. Unkovich, M., Baldock, J. & Farquharson, R. Field measurements of bare soil evaporation and crop transpiration, and transpiration efficiency, for rainfed grain crops in Australia – A review. *Agric. Water Manag.* **205**, 72–80 (2018).
50. Running, S.W. & Zhao, M. Daily GPP and annual NPP (MOD17A2/A3) products NASA Earth Observing System MODIS land algorithm. [https://www.nts.gov/umt.edu/files/modis/MOD17UsersGuide2015\\_v3.pdf](https://www.nts.gov/umt.edu/files/modis/MOD17UsersGuide2015_v3.pdf) (2015).
51. Anwar, M. R., Leary, G. O., McNeil, D., Hossain, M. & Nelson, R. Climate change impact on rainfed wheat in south-eastern Australia. *Field Crops Res.* **104**, 139–147 (2007).
52. Cannon, A. J. Multivariate quantile mapping bias correction: an n-dimensional probability density function transform for climate model simulations of multiple variables. *Clim. Dyn.* **50**, 31–49 (2018).
53. Cannon, A.J. MBC: Multivariate Bias Correction of Climate Model Outputs. <https://CRAN.R-project.org/package=MBC> (2020).
54. Webster, R. & Oliver, M.A. *Geostatistics for Environmental Scientists*, 2nd edition. John Wiley & Sons, Chichester (2007).
55. Quinlan, J.R. Learning with continuous classes. In: *5th Australian joint conference on artificial intelligence*, World Scientific, Singapore, pp. 343–348 (1992).
56. Henderson, B., Bui, E., Moran, C. & Simon, D. Australia-wide predictions of soil properties using decision trees. *Geoderma* **124**, 383–398 (2005).
57. Prescott, J. A. Climatic index for the leaching factor in soil formation. *J. Soil Sci.* **1**, 9–19 (1950).
58. Viscarra Rossel, R. A. Fine-resolution multiscale mapping of clay minerals in Australian soils measured with near infrared spectra. *J. Geophys. Res. Earth Surf.* **116**, 1–15 (2011).
59. Viscarra Rossel, R. A., Brus, D. J., Lobsey, C., Shi, Z. & McLachlan, G. Baseline estimates of soil organic carbon by proximal sensing: Comparing design-based, model-assisted and model-based inference. *Geoderma* **265**, 152–163 (2016).
60. Ziehn, T. et al. The Australian earth system model: Access-esm1.5. *J. South. Hemisph. Earth Syst. Sci.* **70**, 193–214 (2020).
61. Danabasoglu, G. et al. The community earth system model version 2 (CESM2). *J. Adv. Model. Earth Syst.* **12**, 1–35 (2020).
62. Séférian, R. et al. Evaluation of cnrm earth system model, CNRM-ESM2. Role of earth system processes in present-day and future climate. *J. Adv. Model. Earth Syst.* **11**, 4182–4227 (2019).
63. Boucher, O. et al. Presentation and evaluation of the IPSL-CM6a-LR climate model. *J. Adv. Model. Earth Syst.* **12**, 1–52 (2020).
64. Hajima, T. et al. Development of the miroc-es2l earth system model and the evaluation of biogeochemical processes and feedbacks. *Geosci. Model Dev.* **13**, 2197–2244 (2020).
65. Seland, Ø. et al. Overview of the Norwegian earth system model (NorESM2) and key climate response of cmip6 deck, historical, and scenario simulations. *Geosci. Model Dev.* **13**, 6165–6200 (2020).

## Acknowledgements

The Australian Government funded this research through the Australian Research Council's Discovery Projects scheme (ARC project DP210100420) and the Australia-China Science and Research Fund-Joint Research Centres (ACSRF-JRC grant ACSRV000077). The Terrestrial Ecosystem Research Network (TERN) infrastructure, enabled by the National Collaborative Research Infrastructure Strategy (NCRIS), provided the environmental data used in this work.

## Author contributions

R.A.V.R. formulated the research and designed the simulations. M.Z. performed the simulation and with R.A.V.R. and T.B. the data analysis. R.A.V.R. wrote the manuscript with input from R.W., T.B. and M.Z. All authors edited the manuscript. All authors discussed the results and agreed on the final draft.

## Competing interests

The authors declare no competing interests.

## Additional information

**Correspondence** and requests for materials should be addressed to R. A. Viscarra Rossel.

**Reprints and permissions information** is available at <http://www.nature.com/reprints>

**Publisher's note** Springer Nature remains neutral with regard to jurisdictional claims in published maps and institutional affiliations.

**Open Access** This article is licensed under a Creative Commons Attribution 4.0 International License, which permits use, sharing, adaptation, distribution and reproduction in any medium or format, as long as you give appropriate credit to the original author(s) and the source, provide a link to the Creative Commons licence, and indicate if changes were made. The images or other third party material in this article are included in the article's Creative Commons licence, unless indicated otherwise in a credit line to the material. If material is not included in the article's Creative Commons licence and your intended use is not permitted by statutory regulation or exceeds the permitted use, you will need to obtain permission directly from the copyright holder. To view a copy of this licence, visit <http://creativecommons.org/licenses/by/4.0/>.

© The Author(s) 2024